

First principle study of the electronic structure of $\text{Sr}_2\text{FeMoO}_6/\text{SrTiO}_3$ multilayers with and without interfacial Fe deficiency

D. Stoeffler^a

Institut de Physique et de Chimie des Matériaux de Strasbourg (UMR 7504 CNRS -ULP), 23 rue du Loess, BP 43, 67034 Strasbourg Cedex 2, France

Received 10 October 2007 / Received in final form 18 February 2008

Published online 28 March 2008 – © EDP Sciences, Società Italiana di Fisica, Springer-Verlag 2008

Abstract. We investigate the electronic structure of $\text{Sr}_2\text{FeMoO}_6/\text{SrTiO}_3$ (SFMO/STO) multilayers using the ab initio Full Potential Linearized Augmented Plane Wave method in order to study their properties within the GGA and GGA+U methods. We examine more especially the role of the interface on the magnetic and transport properties of these multilayers taking into account a possible Fe deficiency at the interface and we show that bulk behaviour is rapidly recovered due to the strong localization of the interfacial perturbation. For perfect interfaces, the whole structure is found half-metallic within the GGA+U method; the situation being ambiguous within the GGA method where SFMO is at the limit of being half-metallic depending on the structural deformation induced by the STO layer. This leads us to the conclusion that such a system could be used as injection electrode and tunnel barrier in magnetic tunnel junctions with a fully spin polarized injected current. For Fe deficient interfaces, we show that the interfacial densities of states are nearly unpolarized showing that this kind of imperfection has potentially a strong impact on the properties of the multilayers.

PACS. 71.20.-b Electron density of states and band structure of crystalline solids – 71.55.Ak Metals, semimetals, and alloys – 75.47.-m Magnetotransport phenomena; materials for magnetotransport

1 Introduction

The potential use of magnetic half-metal oxide as spin polarization or detection electrode into spintronic devices has stimulated an intense research on the growth of thin films of such ferromagnetic oxides in contact with an ultrathin non magnetic oxide acting as the tunnel barrier. $\text{Sr}_2\text{FeMoO}_6$ (SFMO) double perovskite is one candidate for such kind of materials due to (i) its ferromagnetic ordering up to 415 K and (ii) its predicted half-metallic character i.e. it conducts as a metal for one spin channel and behaves like an insulator for the other one [1,2]. First, epitaxial thin films have been deposited on SrTiO_3 (STO) substrates and it has been shown that they present structural and magnetic properties similar to the bulk material [3–8] confirming its potential. Second, in order to investigate the polarized current outcoming from such SFMO electrodes, magnetic tunnel junctions using an ultrathin STO film as tunnel barrier between SFMO and Co thin layers have been grown [9]. In SFMO/STO/Co junctions,

a clear positive magnetoresistive signal of 50% is obtained at low temperature yielding a negative spin polarization value of 85% for SFMO. This result shows that the SFMO/STO interface preserves a high polarization of the supposed half metallic SFMO electrode. However, it is not clear if there is a lowering of the spin polarization due to the interface with the STO layer or if bulk SFMO has intrinsically this 85% spin polarization.

Experimentally, several studies were focused on $\text{Sr}_2\text{FeMoO}_6/\text{SrTiO}_3$ (SFMO/STO) magnetic tunnel junction but the expected magnetoresistance was not obtained even for well prepared samples [10]. Most of these studies were unable to explain clearly this disappointing result. A depolarization of the current at the interface was finally supposed to be the most reasonable explanation. Recently, by combining X-ray magnetic circular dichroism and X-ray photoemission spectroscopy, it has been shown that the surface magnetic moment of SFMO is anomalously weak and is consistent with a lack of Fe at the surface [10]. The absence of magnetoresistance is consequently ascribed to Fe deficient surfaces and interfaces of the SFMO layer where Fe atoms are replaced by Mo atoms and the

^a e-mail: Daniel.Stoeffler@ipcms.u-strasbg.fr

polarization is strongly reduced over a significant SFMO thickness. The present work investigates the electronic structure and the magnetic properties of SFMO/STO superlattices taking into account such interfacial Fe deficiency. The aim is to examine the occurrence of such an interfacial spin polarization lowering using a first principle method for determining the electronic structure taking electronic correlation into account in the density functional theory within the GGA+U approach (GGA including the semi-empirical Hubbard contribution).

2 Unit cells and calculation method

In the [001] direction, SFMO presents an alternance of FeMoO_4 and Sr_2O_2 atomic layers whereas STO presents an alternance of TiO_2 and SrO atomic layers. Using a $c(2 \times 2)$ cell for STO, by doubling its in plane cell, we get an alternance of Ti_2O_4 and Sr_2O_2 atomic layers similar to the one of SFMO. In order to have the smallest possible SFMO/STO total cell and to insure that the inner atomic plane of each SFMO and STO layer has a bulk-like environment, the total cell is consequently built by juxtaposition of a SFMO layer consisting of $\text{FeMoO}_4/\text{Sr}_2\text{O}_2/\text{FeMoO}_4/\text{Sr}_2\text{O}_2/\text{FeMoO}_4$ stacking (denoted by SFMO_5) and of a STO layer consisting of $\text{Sr}_2\text{O}_2/\text{Ti}_2\text{O}_4/\text{Sr}_2\text{O}_2/\text{Ti}_2\text{O}_4/\text{Sr}_2\text{O}_2$ (denoted by STO_5) directly in contact (see Fig. 1); the denomination of the total cell corresponds then to $\text{SFMO}_5/\text{STO}_5$. Even if the bulk in plane lattice parameters for SFMO and STO are very similar ($a_{\text{SFMO}} = 5.57 \text{ \AA}$, $a_{\text{STO}}\sqrt{2} = 5.52 \text{ \AA}$), the tetragonal distortion resulting from the adjustment of one in plane parameter to the other can play a significant role on the half metallic character of SFMO. Consequently, we consider the two extreme situations i.e. using the in plane parameter of SFMO or STO for the whole stack with a tetragonal distortion applied respectively on the STO or SFMO layer in order to preserve the cell volume. These cells will be used for comparing the results obtained with the GGA and the GGA+U methods.

A larger cell will be used for the investigation of the Fe interfacial deficient case where the interfacial Fe atoms are replaced by Mo atoms; the SFMO₅ layer being replaced by a $\text{AMoO}_4/\text{Sr}_2\text{O}_2/\text{SFMO}_5/\text{Sr}_2\text{O}_2/\text{AMoO}_4$ layer with $A = \text{Fe}$ (perfect interface) or $A = \text{Mo}$ (Fe deficient interface) denoted respectively by $\text{FMO}/\text{SFMO}_7/\text{FMO}$ or $\text{MMO}/\text{SFMO}_7/\text{MMO}$ (see Fig. 1).

The band structure is self-consistently calculated for the considered system in the full potential linearized augmented plane wave formalism (FLAPW) in the FLEUR implementation [14] using the GGA without and with the Hubbard contribution (GGA+U) and taking core, semi-core and valence states into account. For the GGA+U method, we use $U_{\text{Fe}} = 4 \text{ eV}$ as usual in the literature and we set $U = 0$ for all other atoms. All calculations are carried out for a set of increasing \mathbf{k} -points until no variation into the main results is reached. Finally, the densities of states are calculated using a few hundred \mathbf{k} -points.

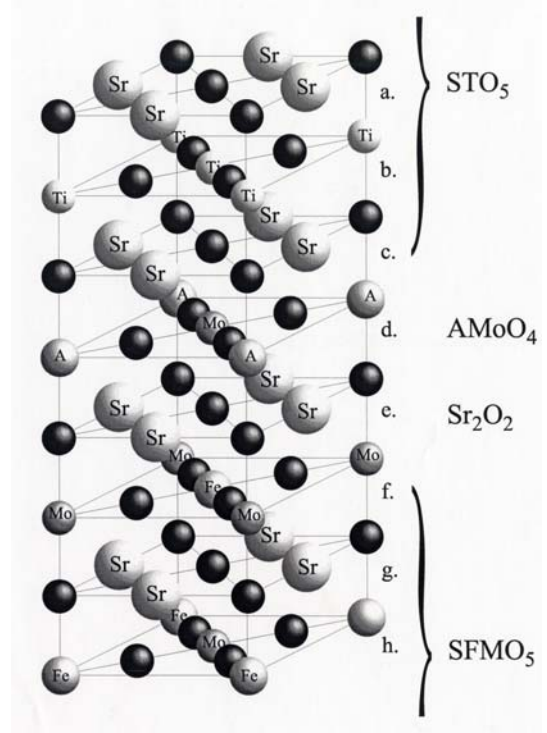


Fig. 1. Schematic representation of half of the $\text{AMoO}_4/\text{Sr}_2\text{O}_2/\text{SFMO}_5/\text{Sr}_2\text{O}_2/\text{AMoO}_4/\text{STO}_5$ cell containing all non equivalent atomic planes labelled from (a). to (h). as in Figures 4 to 7.

3 Comparison between GGA and GGA+U for the stoichiometric case

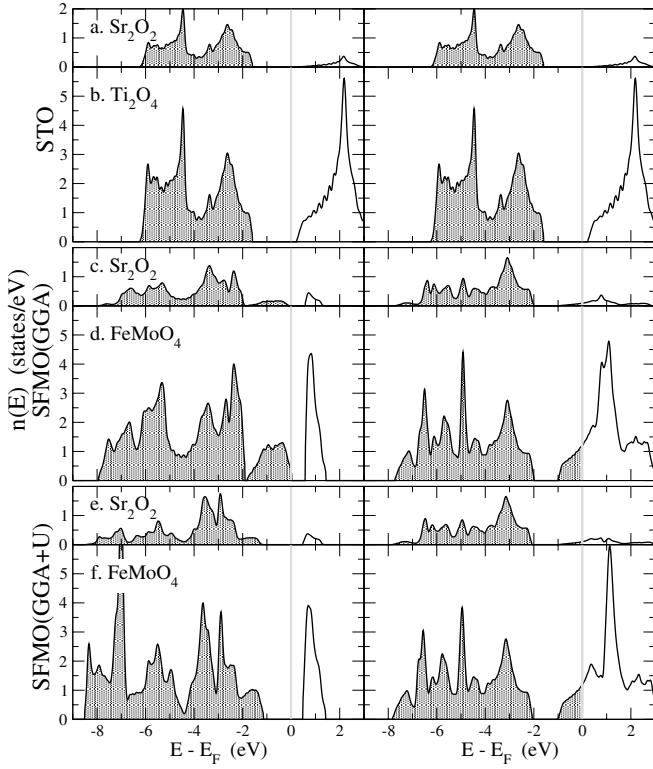
3.1 Bulk-like SFMO and STO

Figures 2 and 3 display the Atomic layer projected densities of states (ALPDOS) for Sr_2O_2 , Ti_2O_4 and FeMoO_4 atomic layer taken bulk-like STO and SFMO using the GGA and GGA+U method for SFMO constrained to the in plane parameter of STO (Fig. 2) and SFMO (Fig. 3). For both STO and SFMO bulk-like system, the resulting tetragonal distortion has a very limited impact on the general electronic structure as exhibited by the APLDOS and the data of Table 1. However, the major difference is found into the top of the valence band of SFMO where some states are shifted to higher energy over the Fermi level. Consequently, with the GGA method, SFMO is no more half metallic when its in plane parameter corresponds to the STO one. This illustrates clearly that the half metallic property of SFMO is not well established with the GGA method: because the Fermi level lies very near the top of the valence band, small variations of the unit cell affects strongly its potential transport properties.

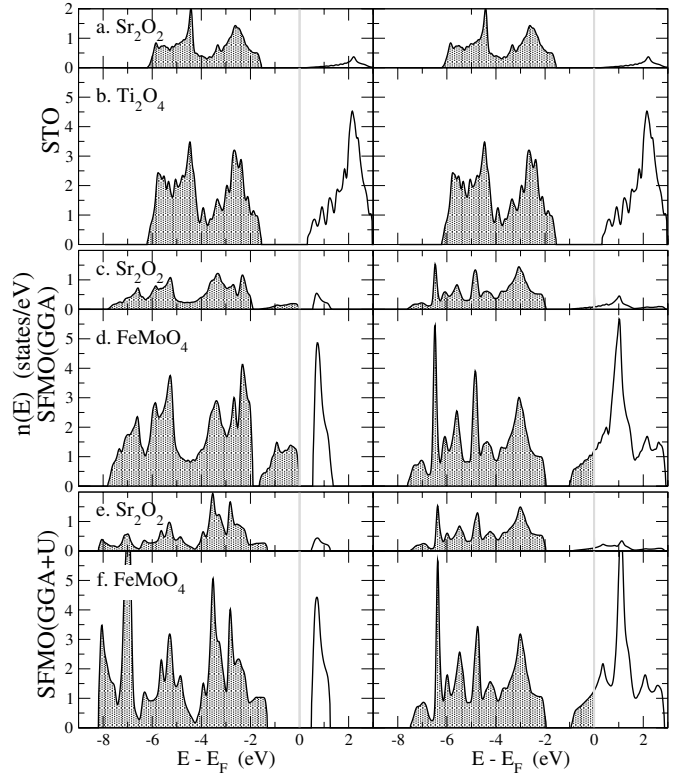
As previously discussed, a reasonable agreement with most experimental findings is obtained when the GGA+U method is used [15]. Moreover, with the GGA+U method, this sensitivity to small cell variations disappears because the energy gap into the majority band around the Fermi level is strongly enhanced. The present work aiming to

Table 1. Calculated band gap, Fe and Mo local moments and total moment for bulk-like SFMO constrained to the in plane parameter of STO or not constrained using GGA and GGA+U methods.

GGA	a (Å)	Gap (eV)	M_{Fe} (μ_B)	M_{Mo} (μ_B)	M_{tot} ($\mu_B/f.u.$)
	$\sqrt{2}a_{\text{STO}} = 5.52$	[0.03, 0.58]	3.76	-0.29	3.98
	$a_{\text{SFMO}} = 5.57$	[-0.02, 0.54]	3.79	-0.29	4.00
GGA+U	a (Å)	Gap (eV)	M_{Fe} (μ_B)	M_{Mo} (μ_B)	M_{tot} ($\mu_B/f.u.$)
	$\sqrt{2}a_{\text{STO}} = 5.52$	[-1.14, 0.48]	3.97	-0.39	4.00
	$a_{\text{SFMO}} = 5.57$	[-1.31, 0.48]	3.97	-0.39	4.00

**Fig. 2.** Atomic layer projected densities of states (ALPDOS) for bulk SrTiO₃ (STO) (a). Sr₂O₂ and (b). Ti₂O₄ atomic layer, obtained with the GGA method for bulk-like Sr₂CoMoO₆ (SFMO) constrained to the in plane cell parameter of STO (see text) (c). Sr₂O₂ and (d). FeMoO₄ atomic layer, obtained with the GGA+U method for bulk-like Sr₂FeMoO₆ (SFMO) constrained to the in plane cell parameter of STO (see text) (e). Sr₂O₂ and (f). FeMoO₄ atomic layer. For STO, the ALPDOS have been shifted to lower energy in order to correspond to the ones in the inner atomic layer of the corresponding STO/SFMO multilayer. The vertical gray line corresponds to the Fermi level (E_F), left and right panels correspond respectively to the up-spin and down-spin ALPDOS.

discuss the perturbation induced by the STO/SFMO interface with and without Fe deficiency on the electronic and magnetic properties of STO/SFMO multilayers, the SFMO in plane parameter will only be considered in the rest of this paper: the changes into the band structure being much more pronounced between the GGA and

**Fig. 3.** ALPDOS for bulk-like STO constrained to the in plane cell parameter of SFMO (see text) (a). Sr₂O₂ and (b). Ti₂O₄ atomic layer, obtained with the GGA method for bulk SFMO (c). Sr₂O₂ and (d). FeMoO₄ atomic layer, obtained with the GGA+U method for bulk SFMO (e). Sr₂O₂ and (f). FeMoO₄ atomic layer. For STO, the ALPDOS have been shifted to lower energy in order to correspond to the ones in the inner atomic layer of the corresponding STO/SFMO multilayer. The vertical gray line corresponds to the Fermi level (E_F), left and right panels correspond respectively to the up-spin and down-spin ALPDOS.

GGA+U results than between the ones for the two in plane parameters.

3.2 SFMO/STO multilayers: GGA method

With this method, as anticipated from bulk ALPDOS, the whole STO/SFMO superlattice is weakly half-metallic

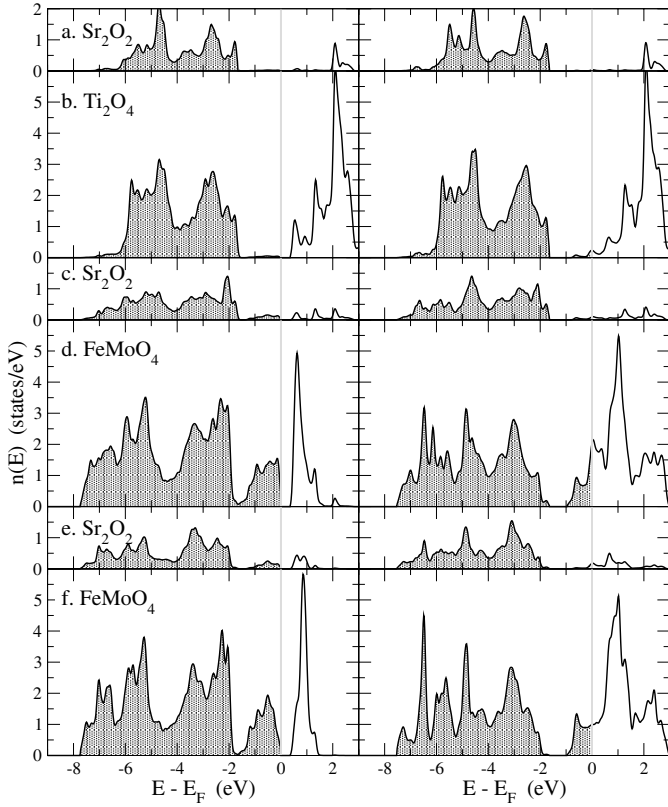


Fig. 4. ALPDOS for SFMO₅/STO₅ constrained to the in plane cell parameter of SFMO (see text) (a). Sr₂O₂ inner STO atomic layer (AL), (b). Ti₂O₄ AL, (c). Sr₂O₂ interfacial AL (d). FeMoO₄ interfacial AL, (e). Sr₂O₂ AL and (f). FeMoO₄ inner AL obtained with the GGA method. The vertical gray line corresponds to the Fermi level (E_F), left and right panels correspond respectively to the up-spin and down-spin ALPDOS.

and a band energy gap, ranging from 0 to 0.3 eV, remains for all ALPDOS (Fig. 4). The STO/SFMO interface has a very limited impact onto the electronic structure of the SFMO even on the interfacial FeMoO₄ atomic layer. This is also reflected in the magnetic moments profile which shows nearly no variation when considering Fe or Mo atoms from the interfacial and from the central atomic planes $M_{\text{Fe}} = 3.78, 3.77\mu_B$ and $M_{\text{Mo}} = -0.29, -0.29\mu_B$ respectively. On the contrary, SFMO induced states appear into a large part of the bulk-like band gap of the majority spin density of states of the STO layer as a consequence of the occurrence of a large number of Fe states for this range of energy. Consequently, if we consider a SFMO/STO/CoFe trilayer where the magnetizations of SFMO and CoFe layers are aligned, the majority spin transmission should be highly asymmetric in small applied voltage (V). When injecting electrons from SFMO to CoFe towards the STO Barrier (for positive V), the majority spin transmission should be very small because no states are available from the SFMO electrode. On the contrary, when injecting from CoFe (for negative V), the majority spin transmission should rapidly increase because a large number of states are directly available below the

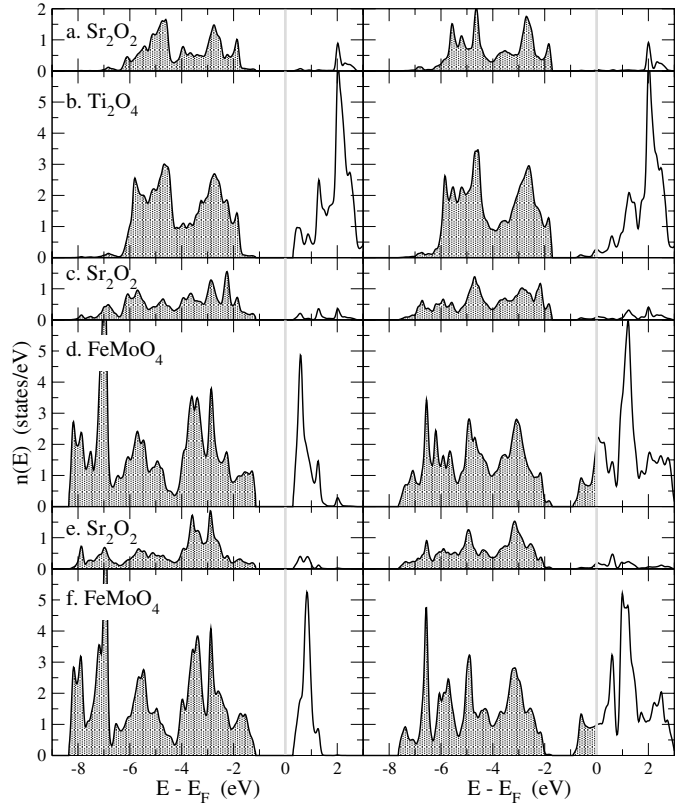


Fig. 5. ALPDOS for SFMO₅/STO₅ constrained to the in plane cell parameter of SFMO (see text) (a). Sr₂O₂ inner STO atomic layer (AL), (b). Ti₂O₄ AL, (c). Sr₂O₂ interfacial AL (d). FeMoO₄ interfacial AL, (e). Sr₂O₂ AL and (f). FeMoO₄ inner AL obtained with the GGA+U method. The vertical gray line corresponds to the Fermi level (E_F), left and right panels correspond respectively to the up-spin and down-spin ALPDOS.

Fermi level. A similar behaviour should also be obtained for a SFMO/STO/SFMO trilayer but with opposite magnetizations of the two SFMO layers.

This transmission asymmetry in applied voltage for one spin channel should be reflected into the total current voltage characteristic and could be a direct proof that the electronic structure of such oxide layers is correctly or not correctly described by the GGA method.

3.3 SFMO/STO multilayers: GGA+U method

With this method, the SFMO/STO superlattice is really entirely half metallic: as displayed in Figure 5, there are no states available around the Fermi level in the majority spin density of states and the energy gaps of both STO and SFMO layer are preserved as a consequence of the very similar gaps (in Fig. 3, the gap of bulk STO ranges from -1.54 to 0.32 eV). Only electrons of the minority spin band can flow through this superlattice which corresponds to the parallel configuration of the magnetization of the two electrodes. For the antiparallel configuration, the gap into the majority band of the electrode with positive magnetization will present some states induced by the

minority states of the next electrode with negative magnetization through the thin STO layer and reciprocally. Consequently, SFMO is no more strictly half-metallic but the current is certainly extremely weak as compared to the one in the parallel configuration because each electrode acts as an insulator in its bulk for one or the other spin channel. The interfacial FeMoO₄ ALPDOS (Fig. 5d) is found very similar to the one of the most central FeMoO₄ atomic layer (which can be considered as bulk-like). Again, this very limited impact of the interface on the properties of the SFMO layer is also reflected in the magnetic moments profile which shows nearly no variation when considering Fe or Mo atoms from the interfacial and from the central atomic planes ($M_{\text{Fe}} = 3.97, 3.99\mu_B$ and $M_{\text{Mo}} = -0.39, -0.39\mu_B$ respectively). Consequently, the STO layer, terminated by the SrO atomic plane, has a weak impact on the electronic structure and the magnetic properties of the SFMO layer.

A high magnetoresistive signal is consequently expected for this case and the current voltage characteristic should be much less asymmetric than for the previous case. This shows clearly that “perfect” SFMO/STO multilayers are a priori good candidates for integration into spintronic devices when their electronic structure can be described with the GGA+U method.

4 Interfacial Fe deficient case

As presented in Section 2, the unit cell is increased by considering a thicker SFMO layer so that two non equivalent FeMoO₄ atomic layers remain when interfacial Fe deficiency will be introduced and only the GGA+U method will be used. For the stoichiometric case, due to the very limited impact of the interface on the properties of the SFMO layer, the present results are very similar to the ones discussed in the previous section: the ALPDOS displayed in Figure 6 are very similar to the corresponding ones of Figure 5 and the magnetic moments profile is very similar too (when considering Fe or Mo atoms from the interfacial to the central atomic planes $M_{\text{Fe}} = 3.99, 3.96, 3.97\mu_B$ and $M_{\text{Mo}} = -0.40, -0.40, -0.37\mu_B$ successively).

Replacing the interfacial Fe atoms by Mo atoms has clearly a strong impact on the global magnetic and transport properties (Fig. 7). Previous works on bulk SFMO with imperfections [11,15] have shown that (i) the half metallic property is lost when Mo antisite are introduced by substituting one of the two Fe atom in a Sr₄FeMo₃O₁₂ cell by a Mo atom and (ii) that the local moment on the Mo antisite is nearly opposite ($+0.26\mu_B$) to the one on the regular Mo sites ($-0.39\mu_B$). However, because this case corresponds to a bulk situation with a high concentration of Mo antisites (half of the Fe sites are occupied by Mo), the role played by such antisites is certainly overestimated.

As displayed by Figure 7, the electronic structure of the SFMO/STO superlattice with Fe deficiency at the interface shows significant differences as compared to the “perfect” case. The half metallic property is lost for the whole cell and the spin polarization of the ALPDOS at the Fermi level, defined by $P = (n^{(+)}(E_F) -$

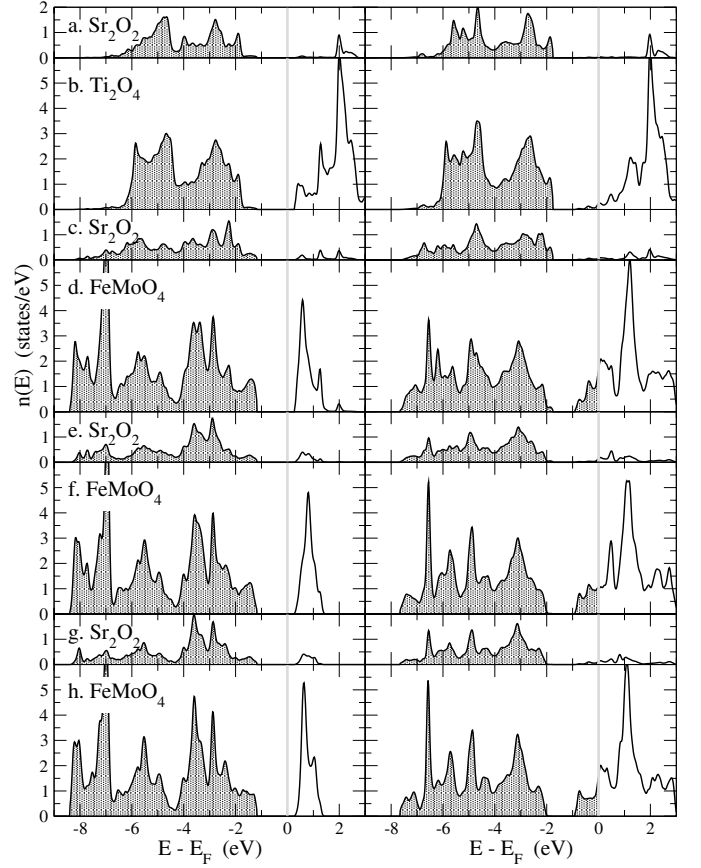


Fig. 6. ALPDOS for SFMO₉/STO₅ constrained to the in plane cell parameter of SFMO (see text) (a). Sr₂O₂ inner STO atomic layer (AL), (b). Ti₂O₄ AL, (c). Sr₂O₂ interfacial AL (d). FeMoO₄ interfacial AL, (e). Sr₂O₂ AL and (f). FeMoO₄ inner AL obtained with the GGA+U method. The vertical gray line corresponds to the Fermi level (E_F), left and right panels correspond respectively to the up-spin and down-spin ALPDOS.

$n^{(-)}(E_F))/(n^{(+)}(E_F) + n^{(-)}(E_F))$, even vanishes completely on the interfacial atomic layer (from the a to the h atomic layer of Figure 7, P is equal to $-0.33, -0.21, +0.01, +0.04, -0.37, -0.45, -0.54, -0.99$). Consequently, for this case, the interface is weakly polarized from the point of view of the spin polarization but also from the point of view of the magnetization (the local moment on the 2 interfacial Mo atoms being equal to $0.15\mu_B$ on the antisite and to $0.04\mu_B$ on the regular site. As clearly exhibited by Figure 7f, the interfacial perturbation of the density of states extends up to the first FeMoO₄ atomic layer: its majority spin density of states presents a peak at the Fermi level being at the origin of the strong reduction of P . For this ALPDOS, as compared to the bulk-like central FeMoO₄ atomic layer for which the gap ranges from -1.20 eV to 0.35 eV, the gap into the majority spin band is clearly partially filled by states ranging from -0.75 eV to 0.30 eV: the ALPDOS corresponding to these states presents 2 peaks which can also be found into the majority spin density of states of the Mo₂O₄ interfacial atomic layer showing clearly that they result from the extension

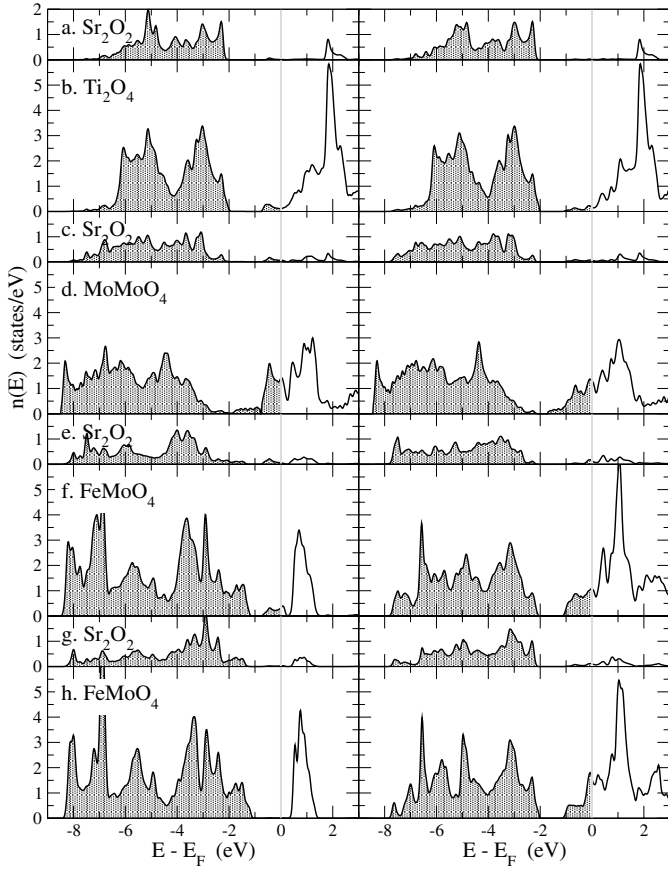


Fig. 7. ALPDOS for SFMO₉/STO₅ presenting Fe deficiency constrained to the in plane cell parameter of SFMO (see text) (a). Sr₂O₂ inner STO atomic layer (AL), (b). Ti₂O₄ AL, (c). Sr₂O₂ interfacial AL (d). MoMoO₄ interfacial AL, (e). Sr₂O₂ AL and (f). FeMoO₄ inner AL obtained with the GGA+U method. The vertical gray line corresponds to the Fermi level (E_F), left and right panels correspond respectively to the up-spin and down-spin ALPDOS.

of the interfacial states due to the Mo antisite. A similar feature is obtained into the Ti₂O₄ density of states of Figure 7b showing that this interfacial states extend on both side of the interface over 5 atomic layers. Consequently, the SFMO/STO interface becomes clearly spin unpolarized when an Fe deficiency is introduced but SFMO recovers rapidly its half metallic feature outside this interface.

5 Discussion

The present band structure calculations show that a lack of Fe atoms at the SFMO/STO interface results in a nearly unpolarized interface in terms of local magnetic moments (the Mo interfacial atoms carry small magnetic moments) and in terms of polarization P which is found nearly equal to zero. This result is in agreement with the experimental one of reference [10] which explains the absence of tunnel magnetoresistance signal in terms of an Fe deficient SFMO surface and interface of SFMO with STO. By comparing the ALPDOS displayed in Figures 7d and 7f. to

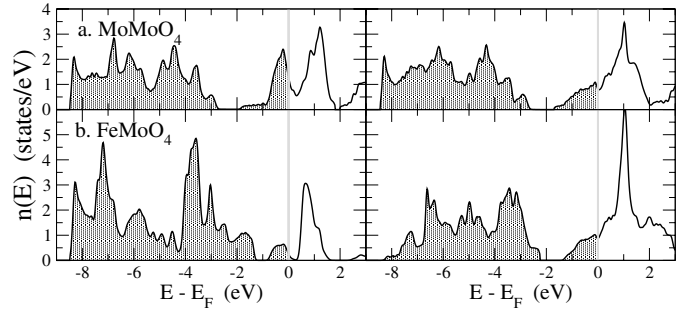


Fig. 8. ALPDOS: for bulk Sr₄FeMo₃O₁₂ (a). MoMoO₂ atomic layer (AL) and (b). FeMoO₄ AL obtained with the GGA+U method. The vertical gray line corresponds to the Fermi level (E_F), left and right panels correspond respectively to the up-spin and down-spin ALPDOS.

the equivalent ALPDOS in a Sr₄FeMo₃O₁₂ cell (Fig. 8), it appears clearly that most of the main features of the density of states are similar confirming that the Ti₂O₄ atomic layer has a limited impact on the electronic structure of the Mo₂O₄ interfacial layer. However, from the viewpoint of the spin polarization, the Fe deficient interface cancels completely P whereas it is only reduced in the bulk Sr₄FeMo₃O₁₂ cell where $P(\text{Mo}_2\text{O}_4) = +0.24$ and $P(\text{FeMoO}_4) = -0.54$. Consequently, when coming from bulk SFMO, the fully polarized current becomes progressively weakly polarized when flowing through the bulk Fe deficient layer (which is modelled here by Sr₄FeMo₃O₁₂) and becomes finally completely unpolarized when reaching the interface. Similarly, for a current flowing into the other direction, after tunneling through STO, it becomes unpolarized at the interface and the resulting current becomes insensitive to the direction of the magnetization in the second SFMO layer. If it is assumed that an intrinsic mechanism (like Fe segregation or evaporation) is at the origin of this interfacial Fe deficiency, this can explain why no tunnel magnetoresistance is observed by most of the groups working on this system and why there has been only one positive result with $P = -0.85$ by Bibes et al. [9]. When considering that only a fraction λ of the interface present this Fe deficiency, the resulting spin polarization can be written as: $P = (\lambda n^{(+)} - (1 - \lambda)n^{(-)} - \lambda n'^{(-)}) / (\lambda n^{(+)} + (1 - \lambda)n^{(-)} + \lambda n'^{(-)})$ where n and n' are respectively the interfacial ALPDOS at the Fermi level for the perfect and the Fe deficient cases. In order to get the measured P value of -0.85 [9] with the present calculated values of the density of states, λ has to be around 0.1 which correspond to only 10% of the interface presenting Fe deficiency. This confirms that Bibes et al. [9], using an improved three-step process growth for the SFMO layer and fabricating nanometer-size tunnel junctions, have effectively reached a high degree of quality of the SFMO/STO interface.

6 Conclusion

To conclude, the present calculations show clearly that perfect SFMO/STO multilayers are half-metallic and that

the SFMO/STO interface becomes spin unpolarized when Fe deficiency occurs at the interface. This conclusion agrees qualitatively with recent experiments which have correlated the lack of measured tunnel magnetoresistance to such an interfacial Fe deficiency [10].

The author thanks S. Colis and A. Dinia for stimulating discussions and the Centre d'Etudes du Calcul Parallèle et de la Visualisation (<http://www-cecpv.u-strasbg.fr>) of University Louis Pasteur for computing facilities.

References

1. K.I. Kobayashi, T. Kimura, H. Sawada, K. Terakura, Y. Tokura, *Nature* **395**, 677 (1998)
2. D.D. Sarma, *Phys. Rev. Lett.* **85**, 2549 (2000)
3. W. Westerburg, D. Reisinger, G. Jakob, *Phys. Rev. B* **62**, R767 (2000)
4. T. Manako et al., *Appl. Phys. Lett.* **74**, 2215 (1999)
5. S.R. Shinde et al., *J. Appl. Phys.* **93**, 1605 (2003)
6. T. Fix et al., *J. Appl. Phys.* **98**, 023712 (2005)
7. S. Colis et al., *J. Appl. Phys.* **98**, 033905 (2005)
8. S. Wang et al., *Appl. Phys. Lett.* **88**, 121912 (2006)
9. M. Bibes et al., *Appl. Phys. Lett.* **83**, 2629 (2003)
10. T. Fix et al., *J. Appl. Phys.* **99**, 08J107 (2006)
11. D. Stoeffler, S. Colis, *J. Phys.: Condens. Matter.* **17**, 6415 (2005)
12. T. Saitoh et al., *Phys. Rev. B* **66**, 035112 (2002)
13. Sugata Ray et al., *Phys. Rev. B* **67**, 085109 (2003)
14. FLEUR is an implementation of the Full Potential Linearized Augmented Plane Wave method freely available at <http://www.flapw.de> funded by the European Research Network Ψ_k and managed by Prof. S. Bluegel
15. D. Stoeffler, S. Colis, *J. Phys.: Condens. Matter* **17**, 6415 (2005)